

Emergent Universal Dynamics for an Atomic Cloud Coupled to an Optical Waveguide

Jan Kumlin,^{1,*} Sebastian Hofferberth,² and Hans Peter Büchler¹

¹*Institute for Theoretical Physics III and Center for Integrated Quantum Science and Technology, University of Stuttgart, 70550 Stuttgart, Germany*

²*Department of Physics, Chemistry and Pharmacy, Physics@SDU, University of Southern Denmark, 5320 Odense, Denmark*

 (Received 23 March 2018; published 2 July 2018)

We study the dynamics of a single collective excitation in a cold ensemble of atoms coupled to a one-dimensional waveguide. The coupling between the atoms and the photonic modes provides a coherent and a dissipative dynamics for this collective excitation. While the dissipative part accounts for the collectively enhanced and directed emission of photons, we find a remarkable universal dynamics for increasing atom numbers exhibiting several revivals under the coherent part. While this phenomenon provides a limit on the intrinsic dephasing for such a collective excitation, a setup is presented where the universal dynamics can be explored.

DOI: [10.1103/PhysRevLett.121.013601](https://doi.org/10.1103/PhysRevLett.121.013601)

The collective interaction between an ensemble of emitters and photons is at the heart of many fascinating phenomena in quantum optics [1,2]. For a single coherent excitation of such an ensemble, the direction and the rate of spontaneous emission are strongly modified and can either be enhanced or suppressed, which has recently been experimentally observed [3,4]. For these effects to be observable, it is crucial that the coherence between the atoms within the ensemble is maintained. While the influence of the thermal motion of atoms has been investigated [5], an ensemble of atoms with a single excitation also exhibits an interaction induced by the virtual exchange of photons [6], which might provide an intrinsic dephasing inherent to any ensemble of emitters. In this Letter, we study within a microscopic analysis whether there is a fundamental limit on this intrinsic dephasing.

Signatures of the coherent interaction by a virtual exchange of photons in an ensemble of atoms with several excitations have been discussed in terms of a collective Lamb shift [6,7], and they have been observed in various physical systems ranging from an ensemble of nuclei [8] over solid-state systems [9,10] to ions [11] and atoms [12,13]. On the theoretical side, recent research has focused on the understanding of the transmission of photons and the appearance of correlations in one-dimensional waveguides [14–19], as well as the appearance of superradiance and a collective Lamb shift in the single-excitation manifold [20–25]. In order to guarantee a single excitation in an ensemble of scatterers, the notion of a superatom has emerged as a powerful concept, where a strong interaction between the excited states restricts suppressed multiple excitations in the ensemble and is conveniently realized with Rydberg atoms [26–33].

Here, we study the influence of the virtual exchange of photons on the properties of such a single collective

excitation, focusing on a setup described by an ensemble of atoms coupled to a one-dimensional waveguide (see Fig. 1). Based on a microscopic analysis, the time evolution of the collective excited state is governed by two competing terms: first, the spontaneous and strongly directed emission into the waveguide, and second, an intrinsic coherent exchange interaction. Remarkably, we find that the coherent part gives rise to a universal dynamics of the collective excitation for increasing particle numbers, and it exhibits several revivals and eventually saturates at a universal value. While this phenomenon provides an intrinsic limit

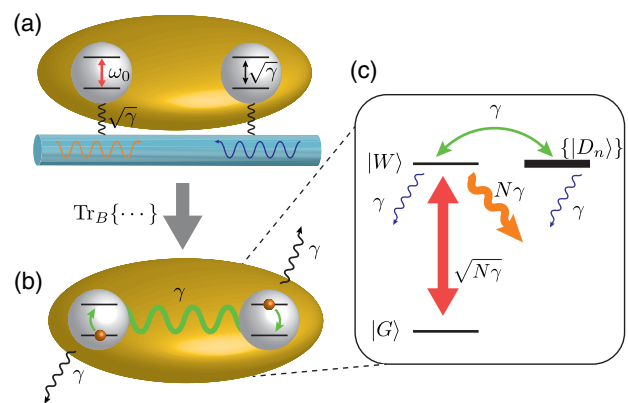


FIG. 1. (a) Two-level atoms coupled to a one-dimensional waveguide with left- and right-moving modes. (b) After integrating out the photonic degrees of freedom, the system exhibits spontaneous emission and an infinite-ranged exchange interaction between the atoms. (c) In the presence of a blockade mechanism, the superatom state $|W\rangle$ is collectively coupled to the ground state with the coupling strength $\sqrt{N\gamma}$ giving rise to an enhanced spontaneous emission $N\gamma$ into the forward direction, while the coherent exchange interaction leads to a coupling between this bright state and the manifold of dark states.

on the dephasing in a superatom, we also present a setup where the universal dynamics can be explored.

Each atom is well-described by a two-level system with the ground state $|g\rangle$ and the excited state $|e\rangle$ (see Fig. 1). The optical transition frequency between the two states is given by $\omega_0 = 2\pi c/\lambda$, with the wavelength λ and the corresponding wave vector $k = 2\pi/\lambda$. In the following, we describe the two states of an atom at position x by the field operators $\psi_g(x)$ and $\psi_e(x)$ for the ground and excited state, respectively. Then, the initial state with all N atoms in the ground state takes the form $|G\rangle = \sqrt{1/N!} \prod_{i=1}^N \psi_g^\dagger(x_i)|0\rangle$. The atomic positions x_i are randomly distributed with a distribution function giving rise to the averaged atomic ground state density $n(x) = \langle G|\psi_g^\dagger(x)\psi_g(x)|G\rangle_{\text{dis}}$; here, $\langle \dots \rangle_{\text{dis}}$ denotes the ensemble average over many experimental realizations. Furthermore, we introduce the operators $S^+(x) = \psi_e^\dagger(x)\psi_g(x)$ creating an excitation from the ground state to the excited state and $S^-(x) = \psi_g^\dagger(x)\psi_e(x)$ for a transition from the excited state to the ground state. These operators satisfy the relation

$$[S^+(x), S^-(y)] = \delta(x-y)[\hat{n}_g(x) - \hat{n}_e(x)], \quad (1)$$

with $\hat{n}_\nu(x) = \psi_\nu^\dagger(x)\psi_\nu(x)$ for $\nu \in \{g, e\}$. Then, the microscopic Hamiltonian describing the coupling of the atoms to a one-dimensional waveguide within the rotating-wave approximation takes the form

$$H = \int \frac{dq}{2\pi} \hbar\omega_q a_q^\dagger a_q + \hbar\omega_0 \int dx \psi_e^\dagger(x)\psi_e(x) - \hbar\sqrt{\gamma} \int dx [\mathcal{E}^\dagger(x)S^-(x) + S^+(x)\mathcal{E}(x)], \quad (2)$$

where $\sqrt{\gamma}$ characterizes the effective mode coupling giving rise to the rate γ for spontaneous emission of a left- or right-moving photon in the waveguide [14–19]. Furthermore, the electric field operator within the waveguide reduces to

$$\mathcal{E}^\dagger(x) = -i\sqrt{c} \int \frac{dq}{2\pi} a_q^\dagger e^{-iqx}. \quad (3)$$

The bosonic operators a_q^\dagger account for the creation of a waveguide mode with momentum q , while $\omega_q = c|q|$ denotes the dispersion relation for the relevant photon modes.

Starting from the microscopic Hamiltonian (2) and integrating out the electric field, the effective dynamics for the atoms alone is governed by a master equation [6,14,34] and takes the form

$$\partial_t \rho = -\frac{i}{\hbar} [H_s, \rho] + \mathcal{D}_F[\rho] + \mathcal{D}_B[\rho]. \quad (4)$$

The first term describes a coherent interaction between the atoms by the exchange of virtual photons,

$$H_s = \hbar\gamma \int dx dy \sin(k|x-y|) S^+(x) S^-(y). \quad (5)$$

The term \mathcal{D}_F (\mathcal{D}_B) describes the spontaneous emission of a photon in the forward (backward) propagating mode, respectively.

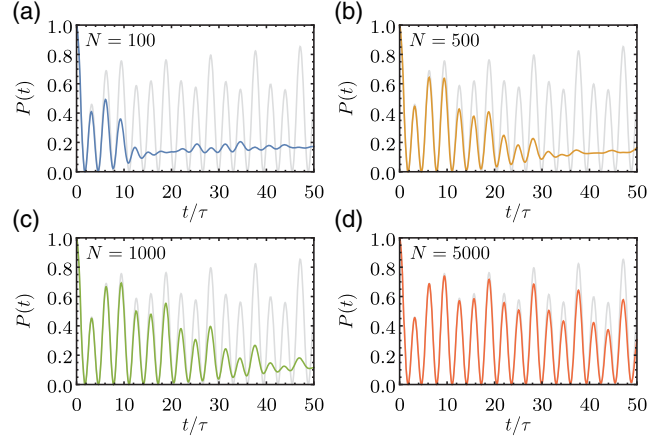


FIG. 2. Time evolution of the state $|W\rangle$ under the Hamiltonian H_s for (a) $N = 100$, (b) $N = 500$, (c) $N = 1000$, and (d) $N = 5000$ particles after averaging over 10^5 realizations with a Gaussian distribution and $k\sigma = 100$. The gray curve indicates the universal dynamics given by Eq. (9).

In the following, the main analysis focuses on the superatom state

$$|W\rangle = \frac{1}{\sqrt{N}} \int dx e^{ikx} S^+(x) |G\rangle, \quad (6)$$

which couples to the incoming light field with the collectively enhanced coupling strength $\sqrt{N}\gamma$. In addition, there are $N-1$ “dark” states $|D_n\rangle = \int dx D_n(x) S^+(x) |G\rangle$, with the wave functions $D_n(x)$ defined by the orthogonality conditions $\langle W|D_n\rangle = 0$ and $\langle D_m|D_n\rangle = \delta_{nm}$.

First, we study the *coherent dynamics* of the state $|W\rangle$ under the Hamiltonian H_s alone. This Hamiltonian gives rise to a coupling between $|W\rangle$ and the dark states $|D_n\rangle$. Therefore, the quantity of interest is the probability $P(t)$ to stay in the superatom state $|W\rangle$ under the coherent time evolution after averaging over many experimental realizations, i.e., $P(t) = \langle \langle W|e^{-iH_s t}|W\rangle|^2 \rangle_{\text{dis}}$. This probability can be evaluated numerically using exact diagonalization and averaging over different disorder realizations, and it is shown in Fig. 2. Remarkably, the dynamics features robust revivals on the characteristic time scale $\tau = \pi/N\gamma$, which only damp out on the slower time scale $\tau_{\text{dp}} = \sqrt{N}\tau$. Therefore, for increasing particle numbers, the amount of observable coherent oscillations increases. Finally, $P(t)$ saturates at a finite value $\sim 1/6$ for long times $t \gg \tau_{\text{dp}}$. Note that, in Fig. 2 we chose a Gaussian density distribution $n(x) = N \exp(-x^2/\sigma^2)/\sqrt{\pi\sigma^2}$; however, the above observations are independent of the atomic density profile as long as the atomic cloud is smooth on distances comparable to the optical wave length λ .

In the following, we provide an analytical analysis of this universal dynamics for the superatom state $|W\rangle$. It turns out to be convenient to split the Hamiltonian $H_s = H_F + H_B$ into two parts, where H_F (H_B) describes the virtual

exchange of forward (backward) propagating photons, respectively. The part describing interaction between the atoms due to forward propagating photons is given by

$$H_F = \frac{\hbar\gamma}{2i} \int dx dy \operatorname{sgn}(x-y) e^{ik(x-y)} S^+(x) S^-(y), \quad (7)$$

and analogously for H_B . These Hamiltonians are exactly solvable [34] and the spectrum takes the form $E_\alpha = (\hbar\gamma/2) \cot(\alpha\pi/2N)$ with α an odd integer and $-N \leq \alpha < N$. Furthermore, the eigenstates are

$$|\alpha, F\rangle = \frac{1}{\sqrt{N}} \int dx e^{ikx} S^+(x) \exp\left(-i\frac{\pi\alpha}{N} F(x)\right) |G\rangle, \quad (8)$$

with the operator $F(x) = \int_{-\infty}^x dz \hat{n}_g(z)$ counting the number of ground state atoms on the left of position x ; similar for $|\alpha, B\rangle$.

For a large atom number $N \gg 1$, only states with $|\alpha| \ll N$ have significant overlap with the superatom state with $|W\rangle = -\sum_\alpha 2/(\pi\alpha) |\alpha, F\rangle$ and the energies reduce to $E_\alpha = N\hbar\gamma/\pi\alpha$. As a result, the probability to remain in the bright state, given only the forward propagating part of the Hamiltonian, is given by $[\chi(t/\tau)]^2$ with $\tau = \pi/N\gamma$ and

$$\chi(s) = \frac{8}{\pi^2} \sum_{n=0}^{\infty} \frac{1}{(1+2n)^2} \cos\left(\frac{s}{1+2n}\right). \quad (9)$$

It is this universal function that $P(t)$ approaches for an increasing number of atoms (see Fig. 2). In order to understand this observation, there are two important points to notice: First, only those states $|\alpha, F\rangle$ with small values of $|\alpha|$ have a significant overlap with $|W\rangle$. In addition, these states dominate the fast dynamical behavior with the characteristic energy scale $E_1 = \hbar\gamma N/\pi$. It is therefore sufficient to restrict the analysis to low values of $|\alpha|$. Second, the states $|\alpha, F\rangle$ with low values of $|\alpha|$ become exact eigenstates of the full Hamiltonian H_s , with energy E_α in the limit of a large particle number $N \rightarrow \infty$ and a smooth atomic density distribution with $\sigma \gg \lambda$. Then, the universal dynamics $P(t) = [\chi(t/\tau)]^2$ is the asymptotic dynamical behavior for large particle numbers. Note that the precise condition of low values of α reduces to $|\alpha| < \sigma/\lambda$ as shown below.

In order to prove the statement that the states $|\alpha, F/B\rangle$ with low values of α become exact eigenstates in the limit $N \rightarrow \infty$ and $\lambda/\sigma \rightarrow 0$, we analyze the wave function overlap between eigenstates of H_F with the eigenstates of H_B , i.e., $h_{\alpha\beta} = \langle \beta, B | H_B | \alpha, F \rangle / E_0 = \langle \beta, B | \alpha, F \rangle / \beta$, and the matrix element $\delta_\alpha = \langle \alpha, F | H_B | \alpha, F \rangle / E_1$. These dimensionless parameters take the form

$$h_{\alpha\beta} = \frac{1}{\beta} \int \frac{dx}{N} e^{2ikx} \langle G | \hat{n}_g(x) e^{-i[\pi(\alpha+\beta)/N]F(x)} | G \rangle, \quad (10)$$

$$\delta_\alpha = \int \frac{dx dy}{2iN^2} \operatorname{sgn}(x-y) e^{2ik(x-y)} \times \langle G | \hat{n}_g(x) \hat{n}_g(y) e^{-i(\pi\alpha/N)(F(x)-F(y))} | G \rangle. \quad (11)$$

In the limit $N \rightarrow \infty$, we can replace the atomic density operator by its averaged expectation value $n(x)$ as the fluctuations in the density vanish with $1/\sqrt{N}$. Then, the overlaps in $h_{\alpha\beta}$ reduce to the Fourier transformation of a smoothly varying function. Therefore, the overlap between states with low numbers of α, β , i.e., $2|k| \gg \pi|\alpha + \beta|/\sigma$, vanishes for $\lambda/\sigma \rightarrow 0$; here, σ denotes the characteristic size of the atomic cloud in general. For example, it vanishes exponentially for a Gaussian density distribution, while for a stepwise atomic distribution, it vanishes as $(\lambda/\sigma)^2$. On the other hand, overlaps with $|\beta| \gtrsim \sigma/\lambda$ are suppressed by the factor $1/\beta$ in Eq. (10). Similarly, the expression for δ_α reduces to $\delta_\alpha = c_0(\lambda/\sigma) + c_1\alpha(\lambda^2/\sigma^2) + \mathcal{O}((\lambda/\sigma)^3)$, with dimensionless parameters c_0 and c_1 of order unity, which only depend on the atomic density distribution $n(x)$. The first term is an irrelevant shift in energy, while the second correction again vanishes as $(\lambda/\sigma)^2$. In conclusion, we have demonstrated that the eigenstates $|\alpha, F\rangle$ with energy E_α become exact eigenstates of the full Hamiltonian H_s for $|\alpha| < \sigma/\lambda$ in the limit $N \rightarrow \infty$ and $\lambda/\sigma \rightarrow 0$.

Next, we analyze the leading correction due to a finite number of particles N in the regime $\lambda \ll \sigma$. The main influence are deviations from the mean density distribution $n(x)$ due to the random distribution of the particles within each experimental realization. These fluctuations lead to fluctuations of $h_{\alpha\beta}$ and δ_α . We illustrate this behavior for the overlap $w_\alpha = \langle \alpha, B | \alpha, F \rangle$. The important quantity is the variance of these fluctuations, i.e., $\Delta w_\alpha = \sqrt{\langle |w_\alpha|^2 \rangle_{\text{dis}} - \langle |w_\alpha| \rangle_{\text{dis}}^2}$, and its leading contribution takes the form $\Delta w_\alpha = 1/\sqrt{N}$. This result is derived using the general relation

$$\langle \hat{n}_g(x) \hat{n}_g(y) \rangle_{\text{dis}} = \frac{N-1}{N} n(x)n(y) + n(x)\delta(x-y), \quad (12)$$

valid for a thermal gas on distances studied in the present setup. Furthermore, the full distribution function for $|w_\alpha|^2$ can be derived (See Supplemental Material [34]), which leads to an exponential distribution with a mean value $1/N$.

The last step to understand the behavior of $P(t)$ is to derive the leading correction to the energies E_α using perturbation theory in the small parameter w_α ,

$$\frac{E_\alpha^\pm}{E_\alpha} = 1 \pm |w_\alpha| \quad \text{with} \quad |\alpha, \pm\rangle = \frac{1}{\sqrt{2}} (|\alpha, F\rangle \pm e^{i\phi_\alpha} |\alpha, B\rangle)$$

and $w_\alpha = |w_\alpha| e^{i\phi_\alpha}$. Therefore, the relevant energies of the Hamiltonian H_s fluctuate within each experimental realization, with a variance $\Delta E_\alpha = E_\alpha/\sqrt{N}$ giving rise to a characteristic dephasing rate $\tau_{\text{dp}} = \pi/\sqrt{N}\gamma$. This observation allows us to derive the leading dynamical behavior

$P(t)$ for the superatom states $|W\rangle$ by performing the average over many different experimental realizations using the knowledge on the distribution function of $|w_\alpha|^2$,

$$\begin{aligned}
 P(t) = & \left\{ \frac{8}{\pi^2} \sum_{n \geq 0} \frac{2}{(2n+1)^2} \cos\left(\frac{t/\tau}{2n+1}\right) \right. \\
 & \times \left[1 - 2f\left(\frac{t}{2\tau_{\text{dp}}(2n+1)}\right) \right] \left. \right\}^2 \\
 & - \frac{16}{\pi^4} \sum_{n \geq 0} \left\{ \frac{2}{(2n+1)^4} \left(\left[1 - 2f\left(\frac{t}{2\tau_{\text{dp}}(2n+1)}\right) \right]^2 \right. \right. \\
 & \left. \left. - \left[1 - f\left(\frac{t}{\tau_{\text{dp}}(2n+1)}\right) \right] \right) \right\}, \quad (13)
 \end{aligned}$$

with $f(x) = xD(x)$ and the Dawson function $D(x) = e^{-x^2} \int_0^x dt e^{t^2}$ with the asymptotic limit $f(x \rightarrow \infty) = 1/2$. The first term in Eq. (13) is a modification of the universal function [Eq. (9)], which now includes damping on a time scale τ_{dp} . For long times $t \gg \tau_{\text{dp}}$, the dynamics saturates at

$$P(t) \xrightarrow{t \gg \tau_{\text{dp}}} \sum_{n=0}^{\infty} \left(\frac{2}{\pi(2n+1)} \right)^4 = \frac{1}{6}. \quad (14)$$

In Fig. 3, we compare the numerically calculated $P(t)$ for $N = 1000$ averaged over 10^5 realizations, with a Gaussian density distribution and $k\sigma = 100$, and $P(t)$ given in Eq. (13), and we find an excellent agreement.

Finally, we analyze the *dissipative dynamics*. The collective enhancement of the coupling between the forward propagating waveguide mode and the $|W\rangle$ state also implies an enhanced spontaneous emission rate $\Gamma_F = N\gamma$ into the forward direction. In turn, the spontaneous

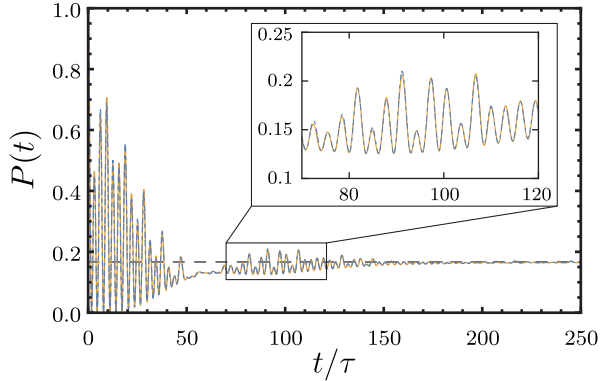


FIG. 3. Comparison between the numerically and analytically calculated time evolution of $|W\rangle$ under H_s . Blue (dashed) curve: Numerically calculated time evolution for $N = 1000$ particles averaged over 10^5 realizations with a Gaussian distribution and $k\sigma = 100$. Orange (solid) curve: Analytical prediction for $\lambda/\sigma \ll 1$ and large N . (Inset): Zoomed image of the dynamics for a better comparison between the numerically and analytically calculated time evolution. Note that there is hardly any visible difference.

emission into the backward propagating mode, Γ_B , depends on the details of the atomic distribution within each experimental realization. In the case of a smooth atomic distribution whose characteristic length scale σ is much larger than the optical wave length λ , the decay rate averaged over many realizations reduces to $\Gamma_B \approx \gamma$, and it accounts for the spontaneous emission of a single atom.

It is important to point out that the characteristic time scale for the revivals in the coherent dynamics and the dissipative part are of the same order. On one hand, we conclude that the coherent part always provides an intrinsic contribution to the dephasing of a superatom state. On the other hand, it is important to disentangle the dissipative dynamics and the coherent part for the experimental observation of the revivals. This goal can be achieved by quenching the spontaneous emission by tailoring the waveguide.

This approach is described in the following for an *experimentally realistic* setup. Such a setup exhibits in addition to the coupling to the waveguide naturally also a spontaneous emission into free space with rate γ_0 . As a first requirement, this decay must be comparable or smaller than the decay into the waveguide, i.e., $\gamma \gtrsim \gamma_0$, which can be achieved in current experimental setups [17,35]. Then, the coherent dynamics, as well as the dephasing, are collectively enhanced and appear on a time scale much faster than residual losses, $N\gamma \gg \sqrt{N}\gamma \gg \gamma_0$. Second, the initial preparation of the setup into the superatom state $|W\rangle$ is achieved using a π pulse with a fast time scale compared to the characteristic dynamics τ . As the Rabi frequency is also collectively enhanced, this condition reduces to $\Omega \gg \gamma\sqrt{N}$, with the single atom Rabi frequency Ω . To bring out the effect of the coherent dynamics, we propose an experimental setup, where the atoms are coupled to a one-dimensional photonic crystal, or Bragg grating, such that the emission process is strongly suppressed due to the opening of a band gap, while the virtual photons mediating the exchange interaction can still propagate outside the photonic band gap. In order to satisfy this condition, the size of the photonic band gap Δ is required to be in the range $\Gamma_F \ll \Delta \ll 2\pi c/\sigma$, where σ is the characteristic size of the system. The lower bound results from the fact that the emitted photon has a Lorentzian spectrum. The upper bound derives from the condition that the virtual photons should be able to propagate with a linear dispersion, such that the initial form of the exchange Hamiltonian is unaffected. For typical quantum optics experiments, the system size is in the micrometer regime which relates to a mode spacing of the virtual photons of a few THz. In addition, the decay into the waveguide is typically in the range of MHz, providing the enhanced decay rate $\Gamma_F = N\gamma$ in the lower GHz regime for $N \sim 10^4$ atoms. This requires the width of the gap to be of the size of a few ten to hundred GHz. Such gratings have been produced, for example, in germanosilicate optical fibers [36], and they have been specifically designed for quantum optics experiments [37].

In conclusion, we demonstrated that the nonequilibrium dynamics of a quantum many-body system, consisting of atoms coupled to a one-dimensional waveguide, can exhibit highly nontrivial universal dynamics characterized by revivals and eventually a saturation on $1/6$. This observation is independent on the averaged atomic distribution $n(x)$, and it becomes more pronounced for increasing particle numbers. In the present analysis, we chose a fixed number of atoms within each experimental realization. However, it is straightforward to derive that for a Poisson distributed number of atoms, the only modification in the dynamics is the enhancement of the dephasing rate by a factor $\sqrt{2}$, while the revivals and the saturation remain unaffected. We expect that similar phenomena can also appear in free space for two-level systems strongly coupled to a single highly focused light mode.

We thank Christoph Tresp for helpful discussions and comments on the manuscript. We thank Christoph Braun and Asaf Paris-Mandoki for discussions at early stages of this work. This work is supported by the European Union under the ERC consolidator grants SIRPOL (Grant No. 681208) and RYD-QNLO (Grant No. 771417), and by the Deutsche Forschungsgemeinschaft (DFG) within the research unit FOR 2247 and the SPP 1929 GiRyd (Project No. HO 4787/3-1).

*kumlin@itp3.uni-stuttgart.de

- [1] R. H. Dicke, *Phys. Rev.* **93**, 99 (1954).
- [2] M. Gross and S. Haroche, *Phys. Rep.* **93**, 301 (1982).
- [3] Y. O. Dudin and A. Kuzmich, *Science* **336**, 887 (2012).
- [4] W. Guerin, M. O. Araújo, and R. Kaiser, *Phys. Rev. Lett.* **116**, 083601 (2016).
- [5] S. L. Bromley, B. Zhu, M. Bishof, X. Zhang, T. Bothwell, J. Schachenmayer, T. L. Nicholson, R. Kaiser, S. F. Yelin, M. D. Lukin, A. M. Rey, and J. Ye, *Nat. Commun.* **7**, 11039 EP (2016).
- [6] R. H. Lehmburg, *Phys. Rev. A* **2**, 883 (1970).
- [7] R. Friedberg, S. Hartmann, and J. Manassah, *Phys. Rep.* **7**, 101 (1973).
- [8] R. Rohlsberger, K. Schlage, B. Sahoo, S. Couet, and R. Ruffer, *Science* **328**, 1248 (2010).
- [9] M. Scheibner, T. Schmidt, L. Worschech, A. Forchel, G. Bacher, T. Passow, and D. Hommel, *Nat. Phys.* **3**, 106 (2007).
- [10] P. Tighineanu, R. S. Daveau, T. B. Lehmann, H. E. Beere, D. A. Ritchie, P. Lodahl, and S. Stobbe, *Phys. Rev. Lett.* **116**, 163604 (2016).
- [11] Z. Meir, O. Schwartz, E. Shahmoon, D. Oron, and R. Ozeri, *Phys. Rev. Lett.* **113**, 193002 (2014).
- [12] J. Pellegrino, R. Bourgain, S. Jennewein, Y. R. P. Sortais, A. Browaeys, S. D. Jenkins, and J. Ruostekoski, *Phys. Rev. Lett.* **113**, 133602 (2014).
- [13] S. Jennewein, M. Besbes, N. J. Schilder, S. D. Jenkins, C. Sauvan, J. Ruostekoski, J.-J. Greffet, Y. R. P. Sortais, and A. Browaeys, *Phys. Rev. Lett.* **116**, 233601 (2016).
- [14] H. Pichler, T. Ramos, A. J. Daley, and P. Zoller, *Phys. Rev. A* **91**, 042116 (2015).
- [15] T. Shi, D. E. Chang, and J. I. Cirac, *Phys. Rev. A* **92**, 053834 (2015).
- [16] J. Ruostekoski and J. Javanainen, *Phys. Rev. Lett.* **117**, 143602 (2016).
- [17] A. Goban, C.-L. Hung, S.-P. Yu, J. Hood, J. Muniz, J. Lee, M. Martin, A. McClung, K. Choi, D. E. Chang, O. Painter, and H. Kimble, *Nat. Commun.* **5**, 3808 (2014).
- [18] P. Solano, P. Barberis-Blostein, F. K. Fatemi, L. A. Orozco, and S. L. Rolston, *Nat. Commun.* **8**, 1857 (2017).
- [19] P. Lodahl, S. Mahmoodian, S. Stobbe, A. Rauschenbeutel, P. Schneeweiss, J. Volz, H. Pichler, and P. Zoller, *Nature (London)* **541**, 473 (2017).
- [20] M. O. Scully, E. S. Fry, C. H. Raymond Ooi, and K. Wódkiewicz, *Phys. Rev. Lett.* **96**, 010501 (2006).
- [21] I. E. Mazets and G. Kurizki, *J. Phys. B* **40**, F105 (2007).
- [22] A. A. Svidzinsky, J.-T. Chang, and M. O. Scully, *Phys. Rev. Lett.* **100**, 160504 (2008).
- [23] M. O. Scully, *Phys. Rev. Lett.* **102**, 143601 (2009).
- [24] J. Javanainen, J. Ruostekoski, Y. Li, and S.-M. Yoo, *Phys. Rev. Lett.* **112**, 113603 (2014).
- [25] A. Asenjo-Garcia, M. Moreno-Cardoner, A. Albrecht, H. J. Kimble, and D. E. Chang, *Phys. Rev. X* **7**, 031024 (2017).
- [26] D. Jaksch, J. I. Cirac, P. Zoller, S. L. Rolston, R. Côté, and M. D. Lukin, *Phys. Rev. Lett.* **85**, 2208 (2000).
- [27] M. D. Lukin, M. Fleischhauer, R. Cote, L. M. Duan, D. Jaksch, J. I. Cirac, and P. Zoller, *Phys. Rev. Lett.* **87**, 037901 (2001).
- [28] M. Saffman, T. G. Walker, and K. Mølmer, *Rev. Mod. Phys.* **82**, 2313 (2010).
- [29] M. Ebert, A. Gill, M. Gibbons, X. Zhang, M. Saffman, and T. G. Walker, *Phys. Rev. Lett.* **112**, 043602 (2014).
- [30] H. Labuhn, D. Barredo, S. Ravets, S. de Léséleuc, T. Macrì, T. Lahaye, and A. Browaeys, *Nature (London)* **534**, 667 (2016).
- [31] Y. O. Dudin, L. Li, F. Bariani, and A. Kuzmich, *Nat. Phys.* **8**, 790 (2012).
- [32] J. Zeiher, P. Schauß, S. Hild, T. Macrì, I. Bloch, and C. Gross, *Phys. Rev. X* **5**, 031015 (2015).
- [33] A. Paris-Mandoki, C. Braun, J. Kumlin, C. Tresp, I. Mirgorodskiy, F. Christaller, H. P. Büchler, and S. Hofferberth, *Phys. Rev. X* **7**, 041010 (2017).
- [34] See Supplemental Material at <http://link.aps.org/supplemental/10.1103/PhysRevLett.121.013601> for details on the derivation and other calculations used in the main text.
- [35] E. Vetsch, D. Reitz, G. Sagué, R. Schmidt, S. T. Dawkins, and A. Rauschenbeutel, *Phys. Rev. Lett.* **104**, 203603 (2010).
- [36] G. Meltz, W. W. Morey, and W. H. Glenn, *Opt. Lett.* **14**, 823 (1989).
- [37] S. P. Yu, J. D. Hood, J. A. Muniz, M. J. Martin, R. Norte, C. L. Hung, S. M. Meenehan, J. D. Cohen, O. Painter, and H. J. Kimble, *Appl. Phys. Lett.* **104**, 111103 (2014).